TOOLING

Self-lubricating CrAlMoN high performance tool coatings for machining of TiAl6V4

K. Bobzin[1] · C. Kalscheuer[1] · M. Carlet[1] · N. Stachowski[1] · W. Hintze[2] · C. Möller[2] · P. Ploog[2]

Abstract

TiAl6V4 allows significant performance improvements in industrial applications. However, the machining is a considerable challenge due to low thermal conductivity, Young's modulus and strong adhesion tendency. This leads to high thermal and mechanical loads on the cutting edge resulting in early tool failure. Today, uncoated cemented carbide tools are commonly used. However, temperature active physical vapor deposition (PVD) coatings like CrAlVN and CrAlMoN provide a promising approach to increase tool life. For this, the coating's ability to form lubricating oxide phases is vital. In the present study, CrAlVN and CrAlMoN coatings were investigated to determine the more suitable version for increasing the economic efficiency of machining TiAl6V4. The coatings were deposited by hybrid direct current magnetron sputtering/high power pulsed magnetron sputtering (dcMS/HPPMS) processes. Morphology, thickness, chemical composition, indentation hardness, indentation modulus and oxide phase composition were analyzed. Moreover, friction and wear behavior of the coated tools were determined using a pin on disc (PoD) tribometer at various temperatures. Additionally, tool life and deformation behavior were analyzed after turning TiAl6V4. The CrAlVN and CrAlMoN coatings show a dense morphology and a smooth surface topography. Both variants have a good adhesion to the cemented carbide tools. For increased temperatures, the tribological analyses showed a reduction in the coefficient of friction. In case of CrAlMoN coated samples, a friction reduction compared to CrAlVN was observed at lower temperatures. Due to this, an increased tool life was achieved for CrAlMoN coated cutting inserts during turning of TiAl6V4.

Keywords Physical vapor deposition · Self-lubrication · Vanadium oxides · Molybdenum oxides · Turning · TiAl64V4

1 Introduction

Titanium alloys, such as TiAl6V4 are frequently used materials in aerospace industries [1]. They enable a significant performance increase due to the combination of a high strength with a low density. Properties of TiAl6V4 include high heat resistance of up to approximately $\vartheta = 550$ °C, low thermal conductivity of $\lambda = 5.8$ W/mK and a Young's modulus of $E = 110–140$ GPa. It is for these properties and the tendency to cause abrasive wear, that titanium alloys are considered to be difficult to machine [2]. Since the heat generated during machining cannot completely dissipate via the chip, the low thermal conductivity leads to high cutting temperatures, leading to temperatures at the cutting edge of 600 °C $\leq \vartheta \leq 750$ °C, depending on cutting parameters and cooling conditions [3]. Furthermore, TiAl6V4 has a strong tendency to chemical reactions with cutting materials. In addition, self-excited vibrations and increased stress concentrations at the cutting edge results from high temperature strength and low Young's modulus [4]. Consequently, high tool wear and build-up edge formation lowers the economic efficiency of machining TiAl6V4. A frequently used approach to increase wear resistance and performance of cutting tools is the use of physical vapor deposition (PVD) or chemical vapor deposition (CVD) coatings. These coatings alleviate the separation of workpiece and tool in order to reduce chemical interaction and cutting forces during the tribological contact in turning processes. A self-lubricating effect due to the formation of easy to shear oxide phases contributes to the decrease of thermal and mechanical loads

✉ N. Stachowski
stachowski@iot.rwth-aachen.de

[1] Surface Engineering Institute (IOT), RWTH Aachen University, Kackertstr. 15, 52072 Aachen, Germany

[2] Institute of Production Management and Technology (IPMT), Hamburg University of Technology (TUHH), Denickestr. 17, 21073 Hamburg, Germany

as well. Self-lubrication oxide phases can be formed under tribological and thermal loads e.g. during machining, by the oxidation of specific transition metals like vanadium or molybdenum. Various self-lubricating oxide phases can be classified as Magnéli phases [5]. To combine self-lubrication effects and wear resistance, the transition metal should be embedded in a nitride hard coating, such as chromium aluminum nitride (CrAlN). In the present study, self-lubricating CrAlMoN and CrAlVN coatings were investigated on cemented carbide tools. Hybrid direct current magnetron sputtering/high power pulsed magnetron sputtering (dcMS/HPPMS) processes were used to deposit both coatings. Coating morphology, thickness, chemical composition, indentation hardness, indentation modulus as well as oxide phase composition were analyzed. Moreover, friction and wear behavior of the coated cutting tools were determined using a pin on disc (PoD) tribometer at $\vartheta = 20\ °C$, $\vartheta = 600\ °C$ and $\vartheta = 800\ °C$ against a TiAl6V4 counterpart. Additionally tool life and deformation behavior of the coated cutting inserts were analyzed after turning of TiAl6V4.

2 Experimental details

2.1 Coating deposition

The coatings were deposited by hybrid dcMS and HPPMS process using an industrial coating unit CC800/9 HPPMS, CemeCon AG, Würselen, Germany. The coating unit is equipped with four dcMS and two HPPMS cathodes. The targets had a size of $A = 500\ mm \times 80\ mm$. Figure 1 shows the target configuration. All coatings were deposited with threefold substrate rotation.

The target material had a purity of $x(Cr) = 99.99\%$, $x(V) = 99.99\%$, $x(Mo) = 99.99\%$ and $x(Al) = 99.50\%$. The plugged targets CrAl20 and VAl20 consisted of a pure base plate with 20 Al plugs (diameter $d = 15\ mm$) each.
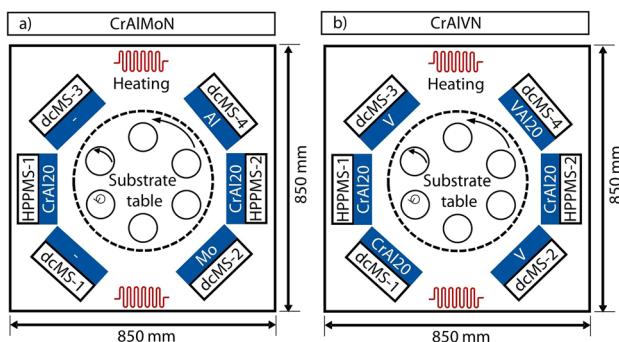

Fig. 1 Schematic representation of the coating unit in top view with two different target configurations for the deposition of CrAlMoN (**a**) and CrAlVN (**b**)

Schematics of the coating architectures for CrAlMoN and CrAlVN coatings are shown in Fig. 2.

Both variants have the same coating architecture and differ only in the chemical composition of the functional layer. The deposition of the CrAl/CrAlN interlayer was performed using the HPPMS cathodes solely. The interlayer is used to achieve a strong adhesion between the carbide substrate and the self-lubricating functional layer. Table 1 shows the process parameters for the deposition of the self-lubricating functional layers.

2.2 Coating characterization methods

To analyze the properties, the coatings were deposited on cemented carbide inserts of grade HW-K10, Kennametal Deutschland GmbH, Rossbach, Germany. The chemical coating composition of aluminum, chromium, molybdenum and vanadium was determined by energy dispersive X-ray spectroscopy (EDS), ZEISS DSM 982 Gemini, Jena, Germany. A quantification of the nitrogen content using EDS was omitted. The coating morphology and thickness were determined using cross-section images obtained from scanning electron microscopy (SEM), ZEISS DSM 982 Gemini, Jena, Germany. The operating voltage for the SEM measurements was $U_S = 4.0\ kV$. EDS and SEM investigations were conducted at the Central Facility of Electron Microscopy (GFE) at RWTH Aachen University. The roughness values Ra and Rz were determined by confocal laser scanning microscopy (CLSM) VK-X 210, Keyence Corporation, Osaka, Japan. Indentation modulus E_{IT} and the indentation hardness H_{IT} were identified by nanoindentation measurements according to DIN EN ISO 14577. For this, a Triboindenter TI 950, Bruker Corporation, Billerica, Massachusetts, USA, with an indentation force of $F = 10\ mN$ was used. In order to avoid an impact on the substrate hardness, the indentation depth was limited to 10% of the coating thickness. Subsequently, the evaluation was conducted according to the strategy of Oliver and Pharr [6]. The Poisson`s ratio was assumed to be $\upsilon = 0.25$. The phase composition in the as-deposited state was investigated by X-ray diffraction using a XRD
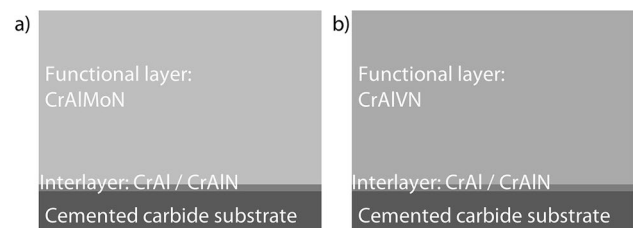

Fig. 2 Schematic representation of the coating architecture of CrAlMoN (**a**) and CrAlVN (**b**)

Table 1 Process parameters for coating deposition

Process parameters	CrAlMoN	CrAlVN
Total pressure p [mPa]	540	560
Argon flow j(Ar) [sccm]	200	200
Nitrogen flow j(N$_2$) [sccm]	Pressure controlled	Pressure controlled
Heating power P$_H$ [kW]	8.0	8.0
Bias voltage U$_{Bias}$ [V]	− 100	− 100
HPPMS 1—target/power P$_{HPPMS-1}$ [kW]	CrAl20/0.5	CrAl20/5.0
HPPMS 2—target/power P$_{HPPMS-2}$ [kW]	CrAl20/3.0	CrAl20/5.0
dcMS-1—target/power P$_{dcMS-1}$ [kW]	–	CrAl20/4
dcMS-2—target/power P$_{dcMS-2}$ [kW]	Mo/1.0	V/4.5
dcMS-3—target/power P$_{dcMS-3}$ [kW]	–	V/4.5
dcMS-4—target/power P$_{dcMS-4}$ [kW]	Al/3.0	VAl20/4.5

3003, GE Energy Germany GmbH, Ratingen, Germany. The evaluations were conducted using Cu-Kα radiation with a wavelength of $\lambda = 0.154$ nm, a voltage of U = 40 kV, a current of I = 40 mA, a diffraction angle of $\omega = 3°$, a step size of s = 0.1° and a step time of t = 5 s. Moreover, the adhesion between coating and cemented carbide sample was evaluated by Rockwell indentation tests according to DIN 4856. For this purpose, a Rockwell tester HP100, Knuth Machine Tools GmbH, Wasbek, Germany, with a normal force of F ≈ 588.4 N (F = 60 kp) was used. Afterwards, the indentation region was analyzed via CLSM to evaluate the adhesion class.

2.3 Tribological behavior

The tribological behavior of the coated cemented carbide samples were tested under continuous sliding conditions in a pin on disc (PoD) tribometer. All tests were conducted under dry conditions in a coating/TiAl6V4 contact at initial Hertzian pressure $p_0 = 1,000$ MPa, calculated based on base and counterpart properties. For the tests, a normal force $F_N = 5$ N, velocity v = 0.1 m/s, radius r = 2.5 mm, distance l = 500 m and a TiAl6V4 pin with spherical tip d = 6 mm was chosen. Test-temperatures were $\vartheta = 20$ °C, $\vartheta = 600$ °C and $\vartheta = 800$ °C with one repetition of each tribological test being performed. The average coefficients of friction (CoF) were evaluated after a running in distance of approximately $l \approx 150$ m between 100 m < l < 500 m. Topography and wear analyses of the wear tracks on the basic parts and wear areas on the counterparts were conducted on one of the two samples after tribological testing by means of CLSM. Furthermore, the surface of the wear tracks were analyzed by Raman spectroscopy using a Raman spectroscope, Renishaw InVia Reflex, Renishaw GmbH, Pliezhausen, Germany, with a $\lambda = 532$ nm laser and a diffraction grating g($\lambda = 532$ nm) = 1800 l/mm. The laser was calibrated using a silicon reference sample.

2.4 Cutting tests

For the cutting experiments, longitudinal turning of TiAl6V4 with a depth of cut of $a_p = 1.2$ mm, a setting angle of $\kappa_r = 95°$, a feed rate of f = 0.12 mm and different cutting velocities used in finish turning, were chosen, see Table 2.

For the cutting tests, a flank wear land width $VB_{max} = 100$ μm and a maximum tool life of T = 20 min are used as tool life criteria. The tests were carried out with CrAlMoN and CrAlVN coated cemented carbide cutting inserts CNGP 120,408 of grade HW-K10, Kennametal Deutschland GmbH, Rosbach, Germany, with a corner radius of $r_\varepsilon = 0.8$ mm, an effective rake angle of $\gamma_{eff} = 2°$, an effective clearance angle of $\alpha_{eff} = 6°$ and a cutting edge radius of $r_\beta = (6+2)$ μm. For reference, the tests were performed with uncoated cutting tools as well. All tests were conducted using cooling emulsion (9%) consisting of deionized water and cooling lubricant B-Cool 675, Blaser Swisslube AG, Switzerland using a CNC lathe MD5S, Gildemeister Drehmaschinen GmbH, Bielefeld, Germany. The CNC lathe was equipped with a dynamometer type 9257B, Kistler Instrumente GmbH, Sindelfingen, Germany, for force measurement. A schematic representation of the experimental setup is shown in Fig. 3.

In order to analyze plastic deformation behavior of the cutting edge as result of thermal and mechanical loads while cutting of TiAl6V4, height profiles of the flank surfaces h_{ce} were measured using an Alicona InfiniteFocus G4, Alicona Imaging GmbH, Graz, Austria, [7]. As shown in Fig. 4, height profiles are measured from the point M_{ce} along the

Table 2 Machining parameters for turning experiments

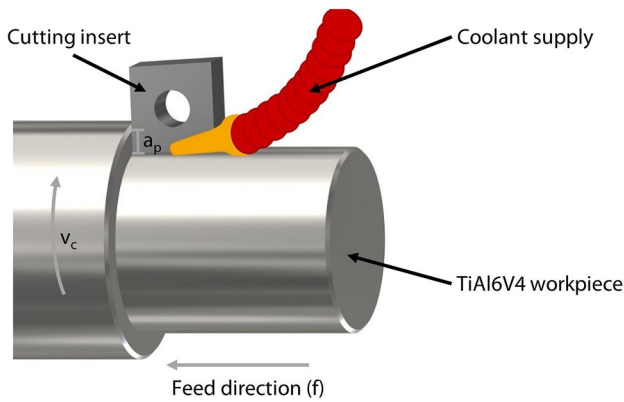| Machining strategy	Depth of cut a_p [mm]	Feed rate f [mm]	Cutting velocity v_c [m/min]	Flank wear land width VB_{max} [μm]
Finish turning	1.2	0.12	65/80	100

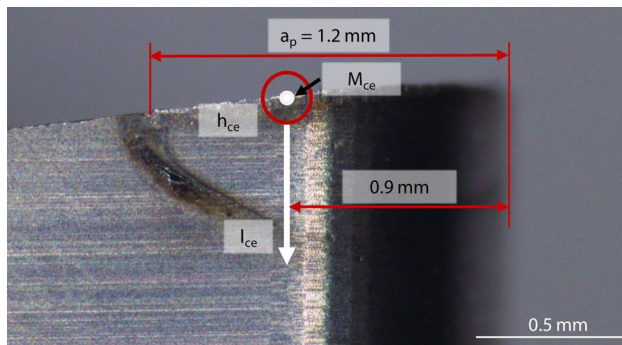**Fig. 3** Schematic representation of experimental setup on CNC lathe used for cutting tests

Fig. 4 Measurement situation for obtaining height profiles on the flank surface of the tested cemented carbide insert

Table 3 Chemical composition of CrAlMoN and CrAlVN after coating deposition by EDS analysis

Coating system	CrAlMoN	CrAlVN
Cr [at.-%]	35	51
Al [at.-%]	39	12
V [at.-%]	0	37
Mo [at.-%]	26	0

path of $l_{ce} = 150$ μm at a distance which represents 75% of the depth of cut $a_p = 1.2$ mm.

3 Results and discussion

3.1 Coating characterization

Table 3 shows the chemical composition of the functional layers from the coatings CrAlMoN and CrAlVN. For the CrAlMoN coating, an aluminum-rich CrAlN was combined
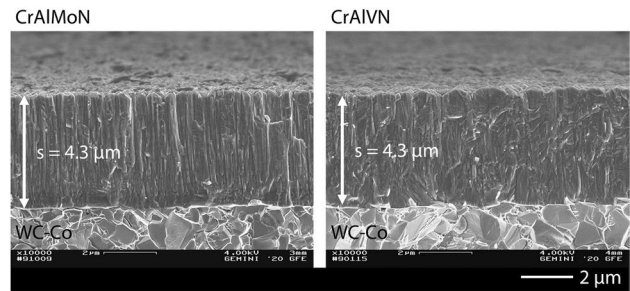
Fig. 5 Cross-section images of CrAlMoN and CrAlVN by SEM
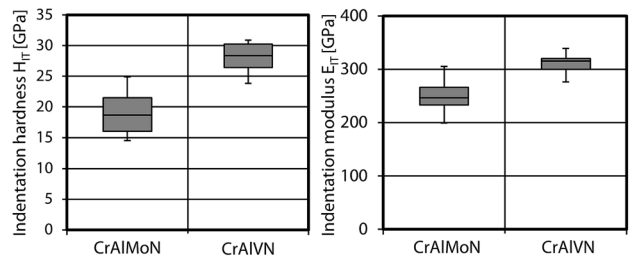
Fig. 6 Indentation hardness and modulus of CrAlMoN and CrAlVN

with molybdenum, which should contribute to the formation of friction-reducing oxide phases. In contrast, the CrAlVN coating combines a chromium-rich CrAlN with the transition metal vanadium. This is motivated by results of preliminary investigations in the context of [8], which had shown that the formation of friction reducing vanadium oxides was enhanced by a low x_{Al}/x_V ratio.

The SEM cross-section images in Fig. 5 show a dense and fine columnar morphology for both coatings with an identical average line roughness of Ra = 0.02 μm for both cases. The measured mean squared roughness for CrAlMoN is Rz = 0.16 μm, thus being slightly increased compared to CrAlVN with Rz = 0.13 μm. The coating thickness of s = 4.3 μm was identical for both sample types.

Nanoindentation measurements were performed to investigate the indentation hardness H_{IT} and the indentation modulus E_{IT}. The results are shown in Fig. 6 and were averaged across 30 indents. Compared to the CrAlVN coating with an average indentation hardness of $H_{IT} = (28 \pm 2)$ GPa, the average indentation hardness H_{IT} of CrAlMoN was significantly lower with $H_{IT} = (19 \pm 3)$ GPa. An identical tendency can be observed for the indentation modulus E_{IT}. Such differences are attributed to the chemical composition and present elements, which can lead to a varying degree of lattice distortion.

In order to analyze the phase composition in the as-deposited state, XRD measurements were carried out. The results are shown in Fig. 7. For both variants, cubic CrN and AlN
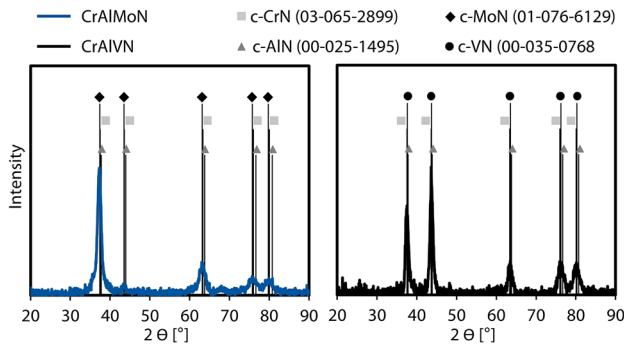
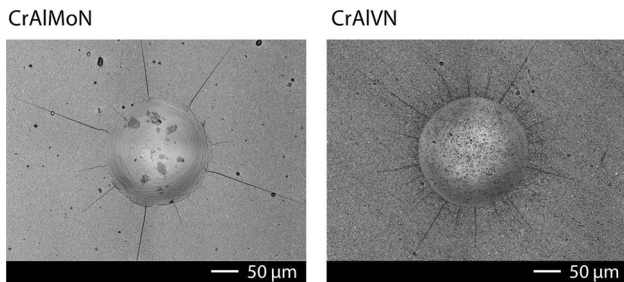**Fig. 7** XRD measurements of CrAlMoN and CrAlVN in the as-deposited state

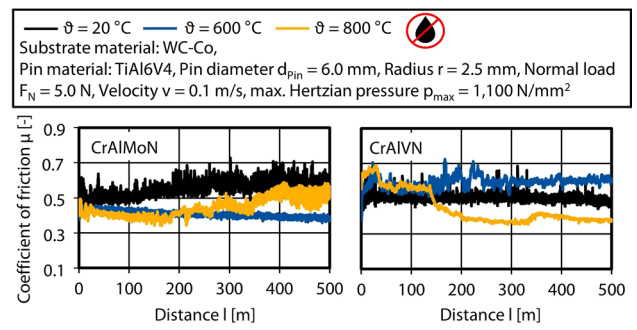**Fig. 9** Coefficient of Friction (CoF) analyses of CrAlMoN and CrAlVN coated cemented carbide substrates against TiAl6V4 using PoD

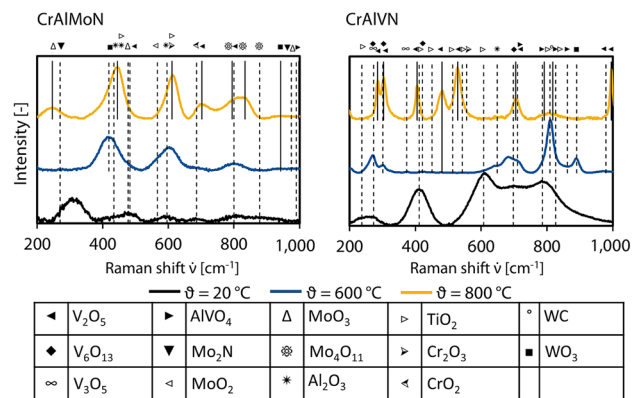**Fig. 8** CLSM micrographs of Rockwell indents of CrAlMoN and CrAlVN on cemented carbide samples

Fig. 10 Raman spectra at the surface of CrAlMoN and CrAlVN after PoD analyses at $\vartheta = 20\,°C$, $\vartheta = 600\,°C$ and $\vartheta = 800\,°C$

peaks were detected. Moreover five typical cubic MoN peaks for CrAlMoN respectively several cubic VN peaks in case of CrAlVN were identified.

The adhesion between coating and cemented carbide sample was evaluated by Rockwell indentation tests according to DIN 4856. Figure 8 shows the CLSM micrographs of these tests on the cemented carbide sample. Except of some radial cracks, no coating delamination could be observed. This indicates a strong adhesion between coating and substrate, which is classified as adhesion class HF 1. Furthermore, the results indicate that the coating is able to withstand a significant plastic deformation of the substrate material without coating delamination. This is crucial during cutting to prevent chipping.

3.2 Tribological behavior

To analyze the friction behavior at different temperatures, tribological PoD-tests were conducted at $\vartheta = 20\,°C$, $\vartheta = 600$ °C and $\vartheta = 800\,°C$, Fig. 9. All following specifications of the coefficient of friction (CoF) were determined after a running-in distance of $l = 100$ m. At $\vartheta = 20\,°C$, the CoF was approximately $\mu \approx 0.55$ for the CrAlVN and $\mu \approx 0.59$ for the CrAlMoN coated samples. After the tests at $\vartheta = 600\,°C$ the CoF appeared higher for the CrAlVN coating. This effect

has already been shown in [9] and is probably caused by the formation of difficult-to-shear oxides, such as AlVO₄. In contrast, the CoF of the CrAlMoN coated samples decreased significantly to $\mu \approx 0.40$. The investigations at $\vartheta = 800$ °C showed, that for the CrAlVN coated samples, the CoF was reduced to $\mu \approx 0.40$ after a running-in distance of approximately $l = 150$ m. In comparison, the coefficient of friction for the CrAlMoN coated tools showed a slight increase to $\mu \approx 0.46$. Therefore, it is deduced that molybdenum containing coatings require lower process temperatures for the formation of friction reducing oxide phases compared to vanadium containing coatings.

Subsequently, an oxide phase analysis using Raman spectroscopy was carried out within the wear track. The graphs obtained after PoD tests at $\vartheta = 20\,°C$, $\vartheta = 600\,°C$ and $\vartheta = 800$ °C are shown in Fig. 10. For both coatings, a wide variety of oxide peaks can be seen after the experiments at $\vartheta = 800$ °C, as presented by the yellow curve. For CrAlVN coated samples, most of them can be assigned to V_2O_5 [10, 11], V_6O_{13} [11], V_3O_5 [11], AlVO₄ [12] and TiO_2 [13]. The TiO_2 detected within the wear track is attributed to the TiAl6V4

counterpart. For the CrAlMoN coated samples, the peaks can be assigned to MoO_3 [14], MoO_2 [14], Mo_4O_{11} [15], Al_2O_3 [16], Mo_2N [17] and WO_3 [18].

In contrast only a few weakly pronounced peaks, mainly the oxide V_2O_5 were identified for the samples coated with CrAlVN after the experiments at $\vartheta = 600\ °C$. Due to it, WC [18] and WO_3, peaks are caused by the cemented carbide substrate. Therefore, the increased friction coefficient at $\vartheta = 600\ °C$ for the CrAlVN coated samples can be explained by the reduced number of lubricating oxide phases. In contrast, after $\vartheta = 600\ °C$, the samples coated with CrAlMoN show an almost identical formation of oxide phases compared to the experiments at $\vartheta = 800\ °C$. Therefore, it seems that CrAlMoN is able to form friction reducing oxide phases at lower temperatures than $(Cr_{51}Al_{12}V_{37})N$. After the experiments at $\vartheta = 20\ °C$, no significant formation of lubricating oxide phases could be detected for both coating systems.

3.3 Cutting tests

To analyze the effect of both coating versions on the wear behavior during cutting TiAl6V4, turning tests were carried out with uncoated cemented carbide inserts tested as reference as well as using the parameters given in Table 2. Figure 11 shows significant differences regarding the developing flank wear land width VB along the cutting time t_c for both cutting velocities. At a cutting velocity of $v_c = 65$ m/min, the uncoated and CrAlMoN coated insert reach the tool life criteria of T = 20 min. The CrAlVN coated insert reaches a cutting time of $t_c \approx 19$ min until a failure at the cutting edge occurred. For $v_c = 80$ m/min the CrAlMoN coated inserts show significantly longer cutting times compared to CrAlVN and uncoated inserts.

For a cutting velocity of $v_c = 65$ m/min, a flank wear land width of VB = 45 μm is measured for the CrAlMoN coated inserts just after start of cutting tests, subsequently increasing slightly to VB ≈ 55 μm over the cutting time of $t_c = 20$
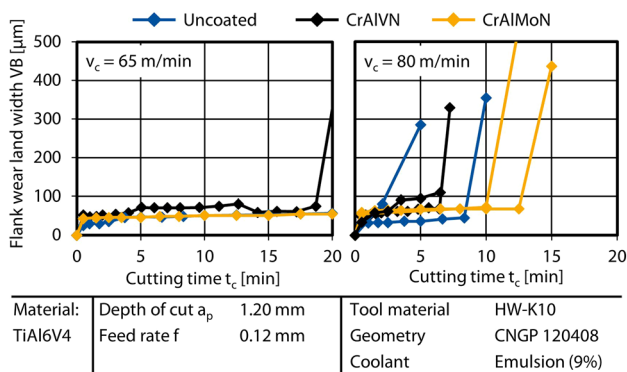
min. For CrAlVN coated cutting insert, a flank wear land width of VB = 50 μm was measured initially after starting the cutting tests and increased to an approximate flank wear land width of VB = 75 μm after a cutting time of $t_c = 19$ min. After a cutting time of $t_c = 18$ min, the cutting edge of the CrAlVN coated insert chipped abruptly. In contrast to the coated samples, the flank wear land width of the uncoated reference reached a flank wear land width of VB = 35 μm after a cutting time of $t_c = 2.5$ min before it slightly increased up to VB = 60 μm at a cutting time of $t_c = 20$ min.

After the cutting tests with a velocity of $v_c = 80$ m/min, the CrAlMoN coated cutting inserts reached a flank wear land width of VB = 65 μm after a cutting time of approximately $t_c = 1.5$ min. Subsequently a slightly increasing up to VB = 70 μm until sudden breakouts of the cutting edge occurred after $t_c = 10.0$ min and $t_c = 12.5$ min. The CrAlMoN coated inserts reached a value of VB ≈ 50 μm just after starting the cutting process. Further on, the flank wear land width increased to approximately VB = 70 μm shortly before cutting edge breakouts at $t_c = 7$ min. The second CrAlVN coated insert reached a VB > 100 μm after $t_c = 6.5$ min. The two uncoated tools showed no uniform process behavior at this cutting velocity. While in the first experiment it reached the lifetime criteria of $VB_{max} = 100$ μm within $t_c = 2.5$ min the second attempt showed an almost similar wear process compared to the coated cutting tools. A slight incrase of flank wear land width up to VB = 45 μm can be observed until $t_c = 8$ min. This is followed by a breakout of the cutting edge. The advantages of coated tools become apparent when comparing the process behavior in machining of TiAl6V4 at increased cutting speeds to the nonuniform wear development of the uncoated cutting tools,. In the test with a cutting velocity of $v_c = 80$ m/min, a significant increase in cutting time t_c can be reached by using molybdenum containing coatings not only compared to the uncoated reference but to the vanadium containing version as well as.

Figure 12 exhibits the development of the wear pattern for the uncoated reference tool, the CrAlVN and the CrAlMoN coated cutting tools. All tools were used at a cutting speed $v_c = 65$ m/min and a feed rate f = 0.12 mm. The wear pattern was recorded at defined steps, being initial state before the cutting tests, after $t_c = 10$ min and $t_c = 20$ min.

A reduced substrate exposure, indicated by less reflections on the cutting edge, of the CrAlVN coated tool compared to the one with molybdenum containing coating, can be observed when comparing the flank wear of both tools after a cutting time of $t_c = 10$ min. Furthermore, this implies that the CrAlVN coating provides a slightly higher resistance to abrasion with slight irregular chipping at the same time.

The brownish area below the cutting edge is less pronounced at the CrAlMoN coated tool. Therefore, it can be deduced that fewer chemical interactions might have
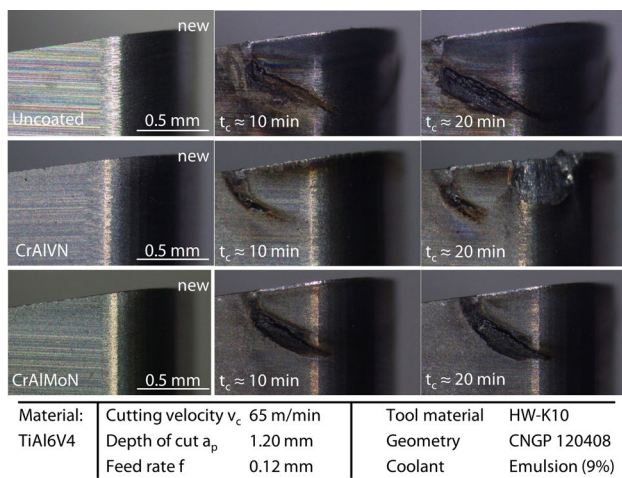
Fig. 11 Flank wear land width VB for varied cutting velocities v_c under constant feed rate of f = 0.12 mm

Fig. 12 Progress of flank wear land widths VB for uncoated, CrAlVN and CrAlMoN inserts at a cutting velocity of $v_c = 65$ m/min
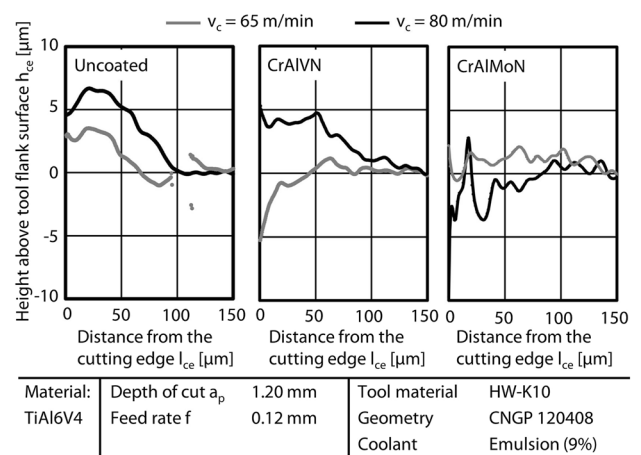

Fig. 13 Height above tool flank surface h_{ce} for cutting velocities $v_c = 65$ m/min and $v_c = 80$ m/min for uncoated, CrAlVN and CrAlMoN coated inserts

occurred just below the cutting edge compared to the CrAlVN coated version.

The flank wear at the cutting edge of both coated tools after $t_c = 10$ min is very similar compared to the one of the uncoated reference tool. Uniform wear with slight chipping of the cutting edge area can be observed for all tools. After a cutting time of $t_c = 20$ min, the smallest increase in wear is observed for the CrAlMoN coated tool, followed by the uncoated reference cutting tool, whereas the CrAlVN coated insert shows a breakout at the cutting edge at this time. For a cutting velocity of $v_c = 80$ m/min, the progress of flank wear land widths appears almost identical until the breakout occurred.

In order to investigate the influence of the coating systems CrAlVN and CrAlMoN on the plastic deformation behavior of the cutting edge, height profile measurements of the inserts across the flank surface were conducted. Figure 13 shows the measured height profiles.

For both coated cutting inserts, no significant plastic deformations at a cutting velocity of $v_c = 65$ m/min were observed. The curve for the height above tool flank surface h_{ce} of the CrAlVN cutting tool showed a negative progression towards the cutting edge. This corresponds with the abrasive tool wear on the flank surface, indicated in Fig. 12. The CrAlMoN coated tool showed a slight plastic deformation with a maximum of $h_{ce} \approx 2$ µm. However, since no clear maximum is evident, the changes are attributed to reaction products with the cooling emulsion visible as brownish surface area in Fig. 12. At a cutting velocity of $v_c = 80$ m/min plastic deformations of $h_{ce} \approx 5$ µm occurred for the CrAlVN coated insert, probably resulting from chipping of the cutting edge before the tool life of $T = 20$ min was reached. For the CrAlMoN coated cutting tool an almost negative progression is visible. The increase at a cutting distance of $l_{ce} = 100$ µm

is again attributed to adhesion processes and chemical reactions. When comparing the plastic deformation of the coated and the uncoated cutting tools obvious differences can be seen. For the uncoated cutting insert, pronounced plastic deformation is visible at the cutting edge. These deformations become more intense with increasing cutting velocity up to a height above flank surface of $h_{ce} \approx 7$ µm at $v_c = 80$ m/min.

4 Conclusions

In order to increase the economic efficiency and tool life while turning titanium alloy TiAl6V4, the use of self-lubricating coating systems based on the formation of lubricating oxide phases while cutting is a suitable approach, resulting in the following findings:

- Tribological analyses using a PoD tribometer showed a reduction in the coefficients of friction for CrAlMoN coated samples already at a temperature of $\vartheta = 600$ °C.
- Raman analyses revealed that friction reducing oxide phases can already be measured at $\vartheta = 600$ °C within the wear track of CrAlMoN coated tools in contrast to those of CrAlVN coated tools under similar conditions.
- CrAlMoN coated tools have a comparatively longer service life of at least 30% at $v_c = 80$ m/min and $f = 0.12$ mm compared to the other variants.
- The plastic deformation behavior of the cutting edge of the coated inserts are lower. This probably results from reduced friction and better load distribution, thus indicating that CrAlMoN coatings are more suitable for the use in machining TiAl6V4, mainly due to self-lubricating oxide phases being already available at lower process

temperatures, which makes them more effective in the machining process.

Declarations

Conflict of interest The authors have no competing interests to declare, that are relevant to the content of this article.

References

1. Veiga C, Davim JP, Loureiro AJR (2012) Properties and applications of titanium alloys: a brief review. Rev Adv Mater Sci 14–34
2. Klocke F (2017) Fertigungsverfahren 1: Zerspanung mit geometrisch bestimmter Schneide. Springer Vieweg, Berlin
3. Krämer A, Lung D, Klocke F (2012) High performance cutting of aircraft and turbine components, in: AIP, pp 425–432
4. Kramer BM, Viens D, Chin S (1993) Theoretical consideration of rare earth metal compounds as tool materials for titanium machining. CIRP Ann 42:111–114
5. Magnéli A (1953) Structures of the ReO 3 -type with recurrent dislocations of atoms: `homologous series' of molybdenum and tungsten oxides. Acta Cryst 6:495–500
6. Oliver WC, Pharr GM (1992) An improved technique for determining hardness and elastic modulus using load and displacement sensing indentation experiments. J Mater Res 7:1564–1583
7. Dahlman P (2002) A comparison of temperature reduction in high-pressure jet-assisted turning using high pressure versus high flowrate. Proc Inst Mech Eng Part B J Eng Manuf 216:467–473
8. Stachowski N, Carlet M, Kalscheuer C, Bobzin K (2021) Oxidation and diffusion behavior of CrAlVN hard coatings for machining Ti6Al4V. In: Behrens B-A, Brosius A, Drossel W-G, Hintze W, Ihlenfeldt S, Nyhuis P (eds) Production at the leading edge of technology, Berlin, Heidelberg
9. Brugnara RH (2016) Hochtemperaturaktive HPPMS-Verschleißschutzschichten durch Bildung reibmindernder Magnéli-Phasen im System (Cr,Al,X)N. Dissertation, Aachen
10. Blume A (2004) Synthese und strukturelle Untersuchungen von Molybdän-, Vanadium- und Wolframoxiden als Referenzverbindungen für die heterogene Katalyse, Technische Universität Berlin
11. Shvets P, Dikaya O, Maksimova K, Goikhman A (2019) A review of Raman spectroscopy of vanadium oxides. J Raman Spectrosc 50:1226–1244
12. Tian H, Wachs IE, Briand LE (2005) Comparison of UV and visible Raman spectroscopy of bulk metal molybdate and metal vanadate catalysts. J Phys Chem B 109:23491–23499
13. Tompsett GA, Bowmaker GA, Cooney RP, Metson JB, Rodgers KA, Seakins JM (1995) The Raman spectrum of brookite, TiO2 (Pbca, Z = 8). J Raman Spectrosc 26:57–62
14. Camacho-López MA, Escobar-Alarcón L, Picquart M, Arroyo R, Córdoba G, Haro-Poniatowski E (2011) Micro-Raman study of the m-MoO2 to α-MoO3 transformation induced by cw-laser irradiation. Opt Mater 33:480–484
15. Dieterle M, Mestl G (2002) Raman spectroscopy of molybdenum oxides. Phys Chem Chem Phys 4:822–826
16. Barshilia HC, Rajam KS (2004) Raman spectroscopy studies on the thermal stability of TiN, CrN, TiAlN coatings and nanolayered TiN/CrN, TiAlN/CrN multilayer coatings. J Mater Res 19:3196–3205
17. Alshibane I (2018) Phase transformations of ternary carbides, nitrides and carbonitrides. Thesis PhD, Glasgow
18. Debus J, Schindler JJ, Waldkirch P, Goeke S, Brümmer A, Biermann D, Bayer M (2016) Indication of worn WC/C surface locations of a dry-running twin-screw rotor by the oxygen incorporation in tungsten-related Raman modes. Appl Phys Lett (109):171601

Publisher's Note Springer Nature remains neutral with regard to jurisdictional claims in published maps and institutional affiliations.